

Chapter 1

Pattern Formation Far From Equilibrium

The diversity of the natural shapes that surround us has a profound impact on the quality of our lives. For this reason alone, it is not surprising that the origins of these shapes have been the subject of serious study since antiquity.¹ It has long been believed that a quantitative characterization of natural forms is an important step towards understanding their origins and behavior. Unfortunately, there have, until recently, been relatively few general approaches towards the quantitative description of the complex, disorderly patterns that are characteristic of most natural phenomena. The essentially non-equilibrium nature of most pattern-formation processes has also contributed to the comparatively slow development of this field. The systematic and generally well understood techniques of equilibrium statistical mechanics cannot be applied to the majority of pattern-formation processes.

In the past one to two decades, the outlook has improved substantially. The pioneering, interdisciplinary work of B. Mandelbrot [2] has demonstrated that mathematical concepts, once believed to be of no possible relevance to the real world, can provide us with new ways of describing and thinking about an amazingly broad range of structures and phenomena. In addition, the scaling concepts that were originally applied to a relatively narrow range of problems such as critical phenomena [3] and the structure of macromolecules [4] have been successfully applied to a very much broader range of problems. In many cases, the fractal geometry approach developed by Man-

1. For example, references to the six-fold form of snowflakes, that go back many centuries, can be found in the commentary by Mason in Hardie's translation of Kepler's work on snowflakes [1].

delbrot can be used to provide a more intuitive, geometric interpretation of scaling behavior. This has brought a measure of intellectual democracy to previously arcane areas of physics and has enabled physicists to contribute to a wide range of important problems outside of the traditional confines of physics.

Many isolated early applications of the fractal approach to physical phenomena can be found. For example, in 1926 Richardson [5] asked the question “*Does the wind possess a velocity?*” and suggested that the distance x traveled by an air “particle” in time t may have to be described “*by something rather like Weierstrass’s function*”

$$x = kt + \sum_n (1/2)^n \cos(5^n \pi t). \quad (1.1)$$

The Weierstrass–Mandelbrot function, a generalization of equation 1.1, described in chapter 2, is now widely recognized as an example of a self-affine fractal function. Richardson went on to describe studies of the dispersion of tracers in the atmosphere and suggested that this process could be described in terms of a length-dependent diffusion coefficient $\mathcal{D}(\ell) \sim \ell^{4/3}$. Richardson argued that the projection of the density of the dispersing tracers onto a straight line $\rho(\ell, t)$ could then be described by the non-Fickian diffusion equation

$$\partial \rho(\ell, t) / \partial t = \partial [\mathcal{D}(\ell) \partial \rho(\ell, t) / \partial \ell] / \partial \ell. \quad (1.2)$$

Richardson showed that the solution to this equation, starting with a delta function distribution at time $t = 0$, has the form

$$\rho(\ell, t) = t^{-3/2} f(\ell^{2/3} / t), \quad (1.3)$$

where $f(x)$ is an exponentially decaying function. It follows, from equation 1.3, that $\langle \ell^2(t) \rangle^{1/2} \sim t^v \sim t^{3/2}$. For a particle moving with a constant velocity, the exponent $1/v$ can be interpreted as a fractal dimensionality. However, for the problem studied by Richardson, space and time are “mixed” so that the exponent relating the distance traveled to the elapsed time cannot be given a simple interpretation in terms of a fractal particle trajectory [6].

Similarly, the development of scaling ideas [3, 4, 7, 8], during the last three decades, has provided new ways of quantitatively describing and better understanding the growth kinetics of both fractal and non-fractal objects. During the same period, a new understanding of non-linear phenomena was developed. The work on non-linear systems demonstrated that apparently complex processes could have simple origins and provided paradigms that helped to motivate the work described in this book.

Fractal geometry has been shown to provide a basis for describing objects as small as polymer molecules and as large as the coastlines of continents.

Mandelbrot [2, 9] has also discussed the application of fractals to the distribution of visible matter in the universe. For some time, it has been accepted that the distribution of visible matter is inhomogeneous and can be described in terms of a fractal dimensionality of $D \approx 1.25$ on “short” length scales, less than the “galaxy correlation length” of about 5 Mpc.² The ideas that there may be no galaxy correlation length and that the distribution might be fractal out to much longer length scales have been the subject of heated controversy. Some aspects of this problem are discussed in chapter 2.

During the past 15 years, the “big bang” theory for the creation of the universe has been seriously challenged by an inflationary model [10, 11, 12] with an inherently fractal nature. This scenario suggests a fractal universe of almost unlimited size.

Most of the applications discussed in this book are much more “down to Earth”. However, it is interesting that theoretical and modeling approaches, similar to those used to simulate non-equilibrium growth and aggregation processes (chapters 3 and 4) and surface growth (chapter 5), have been proposed for the evolution of galaxies [13, 14, 15] and galaxy distributions [16, 17].

While the major applications of fractal geometry have been in the physical and life sciences, many interesting examples have been found that are related to human activities. Examples include the form of urban centers [18, 19], the distribution of weather monitoring stations [20, 21, 22], gravity stations [23, 24] and railroad networks. These fractal distributions did not come about as a result of a design process, but, in some cases, a fractal distribution may be advantageous [25].

It has also been suggested that the distributions of rapidity,³ characterizing the particles generated by high energy collisions, including hadron–hadron, hadron–nucleus and nucleus–nucleus collisions, and cosmic shower events may have a multifractal character [26, 27, 28, 29, 30, 31, 32]. This has been interpreted in terms of a random cascade model [33].

Fractal geometry has also been used to describe the distribution of events in time. In the case of discrete events, the fractal dimensionality D of the set of times $\{t_i\}$ can be measured. Examples of cases in which this approach appears to be of value include the distribution of reversals in the Earth’s magnetic field ($D \approx 0.89$ [34]) and the temporal distribution of earthquakes in a region of limited size ($0.12 < D < 0.26$ [35]).

2. 5 Mpc is 5 megaparsecs, where 1 parsec is the distance at which the mean radius of the Earth’s orbit subtends an angle of 1 second, $1 \text{ pc} \approx 3.2 \text{ light years} \approx 3 \times 10^{16} \text{ m}$.
3. The rapidity y is defined as $y = (1/2) \ln[(E + p_L)/(E - p_L)]$, where E is the energy of an emitted particle and p_L is the component of its momentum along the collision axis. In practice, the pseudo-rapidity, $\eta = -\ln \tan(\theta/2)$, is usually measured, where θ is the emission angle.

1.1 Power Laws and Scaling

Power law relationships play a central role in the study of fractals and scaling. The power law function $y(x)$, given by

$$y(x) = cx^a, \quad (1.4)$$

has an important symmetry that can be expressed as

$$y(\lambda x) = c(\lambda x)^a = c\lambda^a x^a = \text{const.} \cdot y(x). \quad (1.5)$$

This describes the scale invariance of $y(x)$ (the power law function $y(x)$ in equation 1.4 has the same shape on all scales). A trivial, but important, consequence of this scale invariant symmetry is that the exponent a does not depend on the units in which x or y are measured. Functions that satisfy the relationship $y(\lambda x) = \lambda^a y(x)$ are said to be homogeneous. The function

$$y(x) = c_1 x^{a_1} + c_2 x^{a_2} \quad (1.6)$$

does not satisfy equation 1.5 and is an example of an inhomogeneous power law. In practice, the analysis of data from simulations or experiments, in terms of power law exponents, is based on the logarithmic version of equation 1.4

$$\log y(x) = \log c + a \log x, \quad (1.7)$$

so that the exponent a and the amplitude c can be obtained by plotting $\log y(x)$ against $\log x$. The observation of a linear relationship between the logarithms of two quantities over a sufficiently large range of scales is often considered to provide *prima facie* evidence for a power law relationship between these quantities.

In practice, this simple procedure is fraught with hazards. There is no consensus on the standards required for establishing power law relationships from experimental or numerical data. In some areas of physics, it has been possible to observe linear behavior, on a log–log plot, covering more than four orders of magnitude (powers of ten), in both the related quantities. However, data of this quality are quite rare. To observe power law behavior over four decades, from analysis of a recorded image of a physical object, it would be necessary to have a digitized representation with a resolution of better than one part in 10^5 (10^{10} pixels in a 2-dimensional image!). Such images are not routinely available. It would, of course, be possible to extend the range of observation by using images of parts of the structure recorded under different magnifications. If this approach is used, care must be taken to avoid bias towards the selection of “interesting” or even “typical” parts of the pattern.

An important example of a power law relationship is that between the mass M and the characteristic size (average diameter for example) L for a self-similar

fractal aggregate, composed of particles with a diameter ϵ . In this case, the mass of the aggregate is given by

$$M(L, \epsilon) \approx C_0 m(L/\epsilon)^D, \quad (1.8)$$

where m is the mass of a single particle ($m \approx \rho \epsilon^d$, where d is the Euclidean dimensionality of the particle and ρ is the particle density) and C_0 is a geometrical constant of order 1. The exponent D , in equation 1.8, is the fractal dimensionality. Very often, the dependence of the mass on L , when all other quantities are held fixed, is the main focus of interest. In this case, a “shorthand” version of equation 1.8

$$M \sim L^D \quad (1.9)$$

is used. However, it should always be remembered that this equation “stands in” for the dimensionally balanced, or dimensionally homogeneous, equation 1.8. In equation 1.9, and others like it, the symbol “ \sim ” should be interpreted as meaning “scales as”.

This book focuses attention on the power law part of equations like 1.8. In practice, the “amplitude” (c in equation 1.4) is important and embodies the “real physics” behind power law relationships. In many phenomena, the exponents are universal (invariant to small changes in the physical process or model). Under these conditions, the amplitudes provide the only means to control physical properties and behavior. However, important insights can be obtained from the scaling relationships, described by equations such as 1.9. The amplitudes are omitted (some would say perversely) from almost all of the equations in this book, even when they are well known and/or easily calculated. In most cases, it is much more difficult to calculate the amplitude than the exponent. In many practical situations, the scaling relationship $y(x) \sim x^a$ implied by equations such as 1.9 is all that is required. By ignoring the amplitudes, a much broader range of phenomena can be discussed, so that the power and simplicity of the scaling approach is emphasized. The situation here is similar to that encountered in applications of the quantum theory of angular momentum. In this case, the matrix elements needed to calculate properties of physical interest can be divided into two parts, according to the Wigner–Eckart theorem [36, 37]: a part called the reduced matrix element, analogous to the amplitude c in equation 1.4, that depends on the physical details and that is, in most cases, difficult to calculate, and a part that depends only on the angular momentum quantum numbers, which can easily be calculated using group theory.

Phenomena that require the description of the properties of a large ensemble of similar structures, rather than a single sample, are frequently encountered. In this case, equation 1.8 should be replaced by

$$\langle M(L, \epsilon) \rangle \approx C_0 m(L/\epsilon)^D, \quad (1.10)$$

where $\langle M(L, \epsilon) \rangle$ implies averaging the masses of a large number of samples with sizes in a narrow range $L \pm \delta L$, centered on L . This equation, and equations like it, will be replaced by equation 1.9 or $M \sim \epsilon^{-D}$, for clusters with the same overall size composed of monodisperse particles of different sizes ϵ . The notation $\langle \dots \rangle$, to indicate averaging, will appear only if emphasis is required or to avoid ambiguity. The omission of amplitudes and averaging symbols considerably reduces the complexity of equations, and their presence is usually clear from the physical context in which the equations are being used.

Empirical power laws can be expected to arise in two quite different ways. They may be the consequence of a single process that has no inherent length scales, apart from inner and outer cut-off lengths, that define the range over which the power law applies. In this case, robust, homogeneous scaling and universality can be expected. Power law behavior can also arise as a result of many processes, each with its own characteristic length(s). Under these circumstances, relatively weak, non-universal scaling may be expected, and the scaling properties may be inhomogeneous (vary from place to place or time to time, within the same system). An effective power law may also be found as a result of a crossover (slow transition) between two regimes that themselves are characterized by different amplitudes and/or exponents. In practice, it can be difficult to distinguish between these alternatives. However, when a single power law is found over a wide range of scales it is reasonable to take seriously the possibility that a single process, with no inherent length scales, is dominant.

A good example of simple, empirical power law behavior over a large range is provided by studies of impact cratering. In many applications, the cratering efficiency Π_1 , defined as the volume of material removed from the crater divided by the volume of the impacting body, is of central interest. Figure 1.1 shows the dependence of the cratering efficiency on the gravity-scaled yield Π_2 , for transient craters formed by dropping water drops onto water at velocities of $1 - 20 \text{ m s}^{-1}$ and for hypervelocity impacts onto water [38]. The gravity-scaled yield is defined as

$$\Pi_2 = (2g/V^2)(m/\rho)^{1/3} = (2rg/V^2)(4\pi/3)^{1/3}, \quad (1.11)$$

where m is the mass of the impacting body, r is its radius, V is the impact velocity, ρ is the density of the impacting body and g is the acceleration due to gravity. Within a factor of order unity, the dimensionless group Π_2 is equal to $1/\mathcal{F}_1$, where \mathcal{F}_1 , the Froude number, is the ratio between the initial dynamic pressure $V^2\rho$ and the “lithostatic pressure” (hydrostatic pressure in this case) ρ_2gh , where ρ_2 is the “target” density, at a characteristic depth h , equal to the impactor diameter. If the densities ρ and ρ_2 are equal, $\mathcal{F}_1 = V^2/(gh)$.

The data shown in figure 1.1 span almost four decades of velocity, over eight decades in impactor radius (24 decades of mass) and eight decades in gravity. This implies that the dependence of Π_1 on Π_2 can be represented by the power law

$$\Pi_1 \sim \Pi_2^{-a}, \quad (1.12)$$

with $a \approx 0.648$, for a wide range of impact conditions. The cratering efficiency for impacts onto water is determined by the potential energy needed to remove water from the crater. Under these conditions, simple theoretical arguments [45] indicate that, if the cratering efficiency depends only on the kinetic energy of the impactor, then the exponent a should have a value of $3/4$, while if the cratering efficiency depends only on the momentum, then a value of $3/7$ (0.4285...) is predicted. The observed value of about 0.648 can be interpreted in terms of energy coupling or momentum coupling parameters that depend on Π_2 . The momentum coupling parameter is larger than 1, because of the momentum of the material ejected from the crater. Consequently, a crossover from an exponent of $a = 3/4$, at large Froude numbers, to $a = 3/7$, at small Froude numbers, might be expected.

In general, the combination of data from different sources to cover a wide range of scales is a hazardous procedure, since the amplitude c in equation 1.4 may be different for the different sources, even if the exponents are the same. Figure 1.1 combines results from two quite different experiments, using different projectile materials (glass at high velocities and water at low velocities). In this case, the reliability of the results and the quality of the evidence for a single power law rest on the ‘‘Froude scaling’’ used in the data analysis. The evidence for a simple power law, covering the full range of Froude numbers, is compromised by the large gap between the data sets from the hypervelocity impact and low velocity, water drop experiments. The effective exponent of $a \approx 0.648$ could be the result of a slow crossover (chapter 2) from the small Froude number limit to the large Froude number limit. Schmidt and Housen [46] have measured a value of about 0.51 for the exponent a in equation 1.12, for impact cratering in dry, unconsolidated granular materials (sand and iron particles).

A scaling approach, similar to that used for impact cratering, can be used to describe and model explosion cratering. Experiments at normal and elevated gravity [46] indicate that the crater radius r , depth δ and volume \mathcal{V} grow algebraically with increasing time ($r \sim t^b$, $\delta \sim t^{b'}$ and $\mathcal{V} \sim t^{3b''}$, with $b \approx b' \approx b'' \approx 0.36$), at least during the early stages of crater growth, before the effects of gravity or material strength become important. Data from explosion-generated craters in water [46] indicated that $\mathcal{V} \sim t^{3b''}$, with $3b'' \approx 1.07$, over five decades in $\mathcal{V}/\mathcal{V}^*$ and t/t^* , where \mathcal{V}^* and t^* are the final crater volumes and characteristic time, respectively. This value for b'' corresponds to a value of

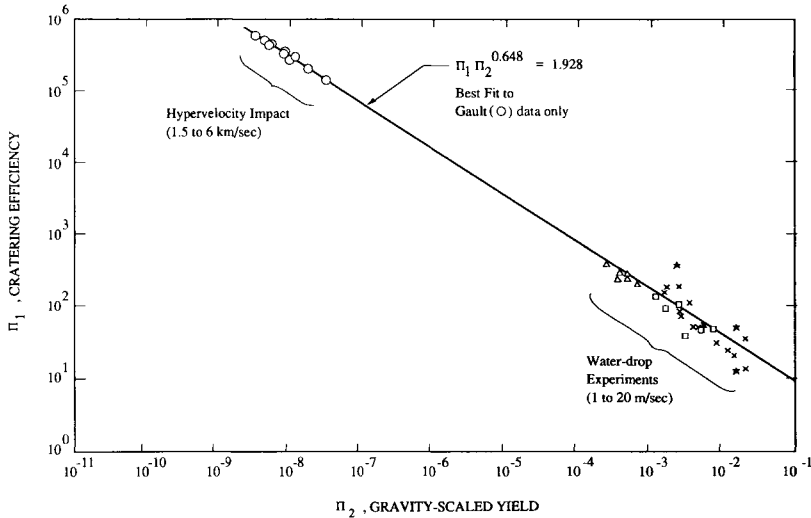


Figure 1.1 Dependence of the cratering efficiency Π_1 on the gravity-scaled yield or inverse Froude number Π_2 , for cratering in water. This figure was provided by K. A. Holsapple. See references [39, 40, 41, 42, 43, 44] for original data.

≈ 0.65 for the exponent a in equation 1.12 ($a = 3\mu/(2 + \mu)$ and $b'' = 3\mu/(1 + \mu)$ [38, 45, 46], where μ is the exponent that relates the far field effects of the impact to the velocity).⁴ For $\mu = 0.55$, $a = 1.65/2.55 = 0.65$ and $b'' = 1.65/1.55 \approx 1.06$.

In the case of impacts onto water or unconsolidated granular material, the size of the crater is limited by the potential energy needed to remove material from the crater. If the target material is a cohesive solid, the mechanical properties of the target will be more important than gravitational effects for small craters. Under these conditions, there will be a crossover from a strength dominated regime for small values of the Froude number to a gravity dominated regime at large Froude numbers [47]. The Froude number at which the crossover takes place depends on the Cauchy number, $C = \rho V^2/Y$, which is the ratio between the dynamic pressure and the material strength Y . In the strength dominated regime, a variety of simulations [47, 48] and theoretical models indicate that the cratering efficiency is related to the projectile velocity by $\Pi_1 \sim V^c$ with $c \approx 1.74$. Again, the measured exponent has a value that is intermediate between the value of $c = 2$ expected if the cratering is dominated by the transfer of kinetic energy and the value of $c = 1$ expected if the cratering is dominated by the momentum of the impactor. At very high velocities, phenomena such as melting of solids and vapor-

4. The magnitude of the effects of the impact can be characterized by the quantity $\mathcal{M} = \rho r^3 V^{3\mu}$, where $3\mu = 2$ if the effects of the impact are determined by the kinetic energy of the impactor alone, and $3\mu = 1$ if the effects of the impact are determined by the impactor momentum alone. These values for μ ($2/3$ and $1/3$, respectively) are limiting values; in practice, effective values lying in the range $1/3 < \mu < 2/3$ have been found to give the best representation of experimental data and simulation results.

ization of liquids and solids become important. The simple empirical power law relationships found at lower velocities cannot be expected to extend to conditions under which these effects become important. A discussion of the understanding of the scaling of impact processes at the time of writing can be found in the review of Holsapple [38] and in a numerical study by O’Keefe and Ahrens [47].

Dimensionless groups, also called dimensionless ratios or dimensionless numbers, play an important role in scaling theory [49, 50, 51]. They can be used to compare systems on very much different time and length scales, and reduce to a minimum the number of variables needed to describe a physical system. If all the relevant dimensionless numbers have the same values, for two different systems, then they will behave in the same way. Such systems are often said to be “similar”. If a system is described by n physical quantities or a model is described by n parameters, or independent variables, then, a property of the system, or a dependent variable, x_0 can be expressed as

$$x_0 = f(\{x_i^{(n)}\}) = f(x_1, x_2, \dots, x_n), \quad (1.13)$$

or

$$F(x_0, \{x_i^{(n)}\}) = F(x_0, x_1, x_2, \dots, x_n) = 0, \quad (1.14)$$

where the set of variables $\{x_i^{(n)}\}$ includes dimensional physical constants such as the acceleration due to gravity g , the mechanical equivalent of heat J and the gas constant R . The physical quantities x_0 and $\{x_i^{(n)}\}$ can be expressed in terms of m “fundamental units” u_1, u_2, \dots, u_m . In the case of a mechanical system, mass, length and time are usually used as the set of fundamental units and $m = 3$. The dimensions $[x_i]$ of the physical quantities x_i have the form

$$[x_i] = u_1^{a_{i,1}} u_2^{a_{i,2}} \dots u_j^{a_{i,j}} \dots u_m^{a_{i,m}}, \quad (1.15)$$

and the dependent variable has the dimensional form

$$[x_0] = u_1^{a_{0,1}} u_2^{a_{0,2}} \dots u_j^{a_{0,j}} \dots u_m^{a_{0,m}}. \quad (1.16)$$

Equation 1.13 can be expressed in terms of dimensionless quantities and written as [49]

$$\Pi_0 = F(\{\Pi^{(l)}\}) \quad (1.17)$$

or

$$\Phi(\Pi_0, \{\Pi^{(l)}\}) = \Phi(\Pi^{(l+1)}) = 0, \quad (1.18)$$

where $\{\Pi^{(l)}\} = \{\Pi_1, \Pi_2, \dots, \Pi_l\}$ is a complete set of dimensionless groups, constructed from the independent variables $\{x^{(n)}\}$, and F is a characteristic function that describes the behavior of the system. In equations 1.17 and 1.18,

Π_0 is a dimensionless property of the system and is the only dimensionless group containing x_0 . The dimensionless groups have the form

$$\Pi_k^{(l)} = x_1^{b_{k,1}} x_2^{b_{k,2}} \dots x_n^{b_{k,n}} \tag{I.19}$$

and

$$\Pi_{(0)} = x_0 x_1^{b_{0,1}} x_2^{b_{0,2}} \dots x_n^{b_{0,n}}, \tag{I.20}$$

so that equation 1.17 can be written as

$$x_0 = (x_1^{b_{0,1}} x_2^{b_{0,2}} \dots x_n^{b_{0,n}})^{-1} F(\{\Pi^{(l)}\}), \tag{I.21}$$

where x_0 and $(x_1^{b_{0,1}} x_2^{b_{0,2}} \dots x_n^{b_{0,n}})^{-1}$ have the same units, and $F(\{\Pi^{(l)}\})$ is dimensionless.

The dimensionless groups are independent of each other in the sense that one dimensionless group cannot be expressed in terms of a product of powers of the others. In most cases, the number of dimensionless groups, $L = l + 1$, in an equation describing the relationship between physical properties (an equation like equation 1.17) is given by $L = l + 1 = n + 1 - m$ or $l = n - m$.⁵

In many problems, there is no natural distinction between dependent and independent variables, and equation 1.18 can be written as

$$\Phi(\{\Pi^{(L)}\}) = \Phi(\Pi_1^{(L)}, \Pi_2^{(L)} \dots \Pi_k^{(L)} \dots \Pi_L^{(L)}) = 0. \tag{I.22}$$

In this case, it is common to construct the set of dimensionless groups $\{\Pi^{(L)}\}$ so that $\Pi_1^{(L)}$ is the only member of the set that contains the variable that is selected as the dependent variable.

The choice of fundamental units is arbitrary [49, 50, 51]. Both the number and nature of the fundamental units can be changed. For example, mass, length and time can be replaced by force, length and time, or the number of fundamental units can be increased by using mass, length, force and time. The number of fundamental units can also be increased by adding units such as temperature or electromagnetic quantities. This does not change the number of dimensionless groups l in $\{\Pi^{(l)}\}$, since addition of a new fundamental unit also adds a new member to the set $\{x_i^{(n)}\}$ of physical quantities (n increases by one). For example, if units of thermal energy are added to the set of units $\{u_j^{(m)}\}$ ($m \rightarrow m + 1$) then the mechanical equivalent of heat J must be added to the set of physical quantities $\{x_i^n\}$, so that $n \rightarrow n + 1$ and $l = n - m$ remains unchanged. If units of temperature are also added to $\{u_j^{(m)}\}$ then the Boltzmann constant k_B must be added to the set $\{x_i^{(n)}\}$, and the number of independent dimensionless groups is again unchanged. Similarly, if the number of fundamental units is decreased, the number of physical parameters is decreased correspondingly. In general, the

5. In general, the number of dimensionless groups is given by $l = n - r$, where r is the rank (the maximum number of independent rows or columns) of the matrix \mathbf{A} of the coefficients $a_{i,j}$ in equation 1.15, with n rows and m columns [50].